default medium (DDM) for 10 days (Fig. 1A). We monitored *Sox1*-GFP expression and neuronal differentiation (as judged by Tuj1 immunostaining) each day during this period. We found that 46C mESCs differentiated more slowly into the neural lineage in DDM than in N2/B27. Although *Sox1*-GFP-positive NPCs could already be observed from differentiation day 3, they reached 80% of the total cell population only after differentiation day 8 (Fig. 1B, D, D′, F and F′). We also observed that starting from differentiation day 4, some of the NPCs had already differentiated into neurons (Fig. 1B, E, E′, F and F′).

We next examined the effects of the Shh inhibitor cyclopamine on 46C mESC survival and neural commitment. mESC-derived NPCs in DDM reportedly tend to possess ventral forebrain-like identity, and the addition of cyclopamine converts most of them into dorsal forebrain-like cells without affecting their proliferative pattern (Gaspard et al., 2008). We observed a similar pattern of neural commitment when we cultured 46C mESCs in DDM with or without cyclopamine, and found no significant difference in terms of cell survival (Fig. 1C, G–I and G′–I′). Thus, we conclude that 46C mESCs can survive and differentiate into the neural lineage in DDM with cyclopamine.

3.2. VPA enhances neurogenesis of 46C mESC-derived NPCs

Another advantage of using 46C mESCs is the existence of an internal ribosome entry site (IRES)-linked puromycin resistance gene which was also knocked-in together with GFP-encoding sequence to replace the *Sox1* gene's open reading frame (Ying et al., 2003). Hence, we can enrich the resulting NPCs by addition of puromycin to the medium. Because we found that the majority of 46C mESCs (>80%) had already differentiated into NPCs by differentiation day 8 (Fig. 1B and C), we added puromycin from differentiation day 8 to day 10 for our subsequent analysis.

Next, we examined the differentiation potential of enriched NPCs which were derived from 46C mESCs. We adopted the differentiation protocol of Gaspard et al. (2008, 2009) for making cortical neurons (Figs. 2A and 3A). At differentiation day 14 (Fig. 2A), we found that more than 80% of the cells were nestin- and Pax6-positive, indicating that they were mostly still NPCs (Fig. 2B and C). VPA treatment for 2 days reduced the proportion of cells positive for both markers (Fig. 2B and C). This reduction was accompanied by an increase of Map2ab- and Tuj1-positive neuronal cells (Fig. 2D and E). We then conducted the same analysis for a longer culture period, up to differentiation day 21 (Fig. 3A). We still found higher proportion of neuronal marker-positive (Map2ab+, Tuj1+) cells in the VPA-treated dishes compared with control (Fig. 3B and C). These results indicate that the enrichment of NPCs by puromycin was successful and that VPA treatment enhances neuronal differentiation of these NPCs.

3.3. VPA induces the generation of superficial-layer neurons

Given that neurogenesis was enhanced by VPA treatment, we then looked at the cortical types of these neurons at differentiation day 14 (after two days exposure to VPA; Fig. 2A). We first found a decreased proportion of early born and deep-layer neuron markers. The proportions of reelin- and Ctip2-positive cells among Tuj1-positive cells were significantly decreased by VPA treatment (Fig. 4A and C). Next, we found an increased proportion of superficial-layer marker (Cux1)-positive cells among Map2ab-positive cells after VPA treatment (Fig. 4B and D). When we prolonged the culture until differentiation day 21 (Fig. 3A), we obtained similar results. The proportions of cells positive for early born or deep-layer markers (reelin+, Ctip2+) among Tuj1-positive neuronal cells were still lower (Fig. 5A and C), while that for cells expressing the superficial-layer marker (Cux1+) was also higher, after VPA treatment (Fig. 5B and D).

When we compared the proportions of neurons in control and VPA-treated cell populations at day 14 with those at day 21, we saw a 3-fold increase during this period under both conditions (Figs. 2E and 3C). In control cells, we observed an increased proportion of Ctip2-positive cells among Tuj1-positive cells during this period (Figs. 4C and 5C). In contrast, the proportions of reelin- or Cux1-positive cells among neuronal marker-positive cells remained unchanged (Figs. 4C and D and 5C and D). These results indicate that in control cells, the majority of neurons produced during this period were Ctip2-positive, even though some of the NPCs still generated reelin- and Cux1-positive neurons.

On the other hand, the proportion of cells positive for the cortical markers we tested among neuronal marker-positive cells after VPA treatment did not change during the extended culture period (Figs. 4C and D and 5C and D). This indicates that VPA enhanced the production of Cux1-positive neurons only while it was being applied to the culture (differentiation day 12 to day 14). Nevertheless, the production of Ctip2-positive neurons in VPA treatment diminished compared to that in control cells during the extended culture period. These results suggest that transient VPA treatment enhances the temporal progression of some deep-layer-producing NPCs into superficial-layer-producing types during the treatment period, whereafter the residual NPCs retain this temporal progression even when VPA has been withdrawn from the culture.

4. Discussion

The brains of mammals differ in many aspects from those of other vertebrates. Most striking among the features that mammals have acquired during evolution are the increased size and complexity of the cerebral cortex, the largest brain structure where many of the higher cognitive functions reside (Finlay and Darlington, 1995; Hill and Walsh, 2005). The mammalian cerebral cortex is highly organized, with a six-layered structure that contains early-born or deep-layer (layers I, V and VI) and superficial-layer neurons (layers II–IV) that are produced in an orderly inside-out fashion (Molyneaux et al., 2007). The increased size and complexity partly reflect the overrepresentation of superficial-layer neurons, which are very abundant in primates, and especially so in human (Marin-Padilla, 1992). These cortical neurons are mainly of two types: pyramidal projection neurons, which mostly originate from NPCs of the dorsolateral wall of the telencephalon (Molyneaux et al., 2007), and interneurons, which originate from the ventral telencephalon during embryonic development (Wonders and Anderson, 2006). Although several studies have reported that ESCs can recapitulate

Fig. 2. VPA enhances neurogenesis of 46C mESC-derived NPCs. (A) Timeline of the corticogenesis protocol used for early differentiation analysis. mESCs were routinely propagated and passaged to gelatin-coated dishes in embryonic stem cells medium (ESM) 1 day before neural induction (day −1). The next day (day 0), medium was changed to chemically defined default medium (DDM) and cyclopamine was added from differentiation day 2 to day 10. At differentiation day 12, mESC-derived NPCs were replated to polylysine/laminin-coated dishes in N2/B27 (1:1 mixture of DDM and Neurobasal + B27). Valproic acid (VPA) was added where appropriate at differentiation day 12 and cells were harvested at differentiation day 14. (B–E) Representative immunostaining images from differentiation day 14 of nestin- and Pax6-expressing (green and red, respectively, in B), or Map2ab- and Tuj1-expressing (green and magenta, respectively, in D) cells and their quantification (C and E). Merged images with and without Hoechst (blue in B and D) are also shown. Tuj1 images in D were derived from the triple immunostaining data of Fig. 4A. Data are mean ± SD from at least three independent experiments. *$P < 0.05$ (Student's *t*-test). Scale bar is 100 μm. (For interpretation of the references to color in this figure legend, the reader is referred to the web version of the article.)

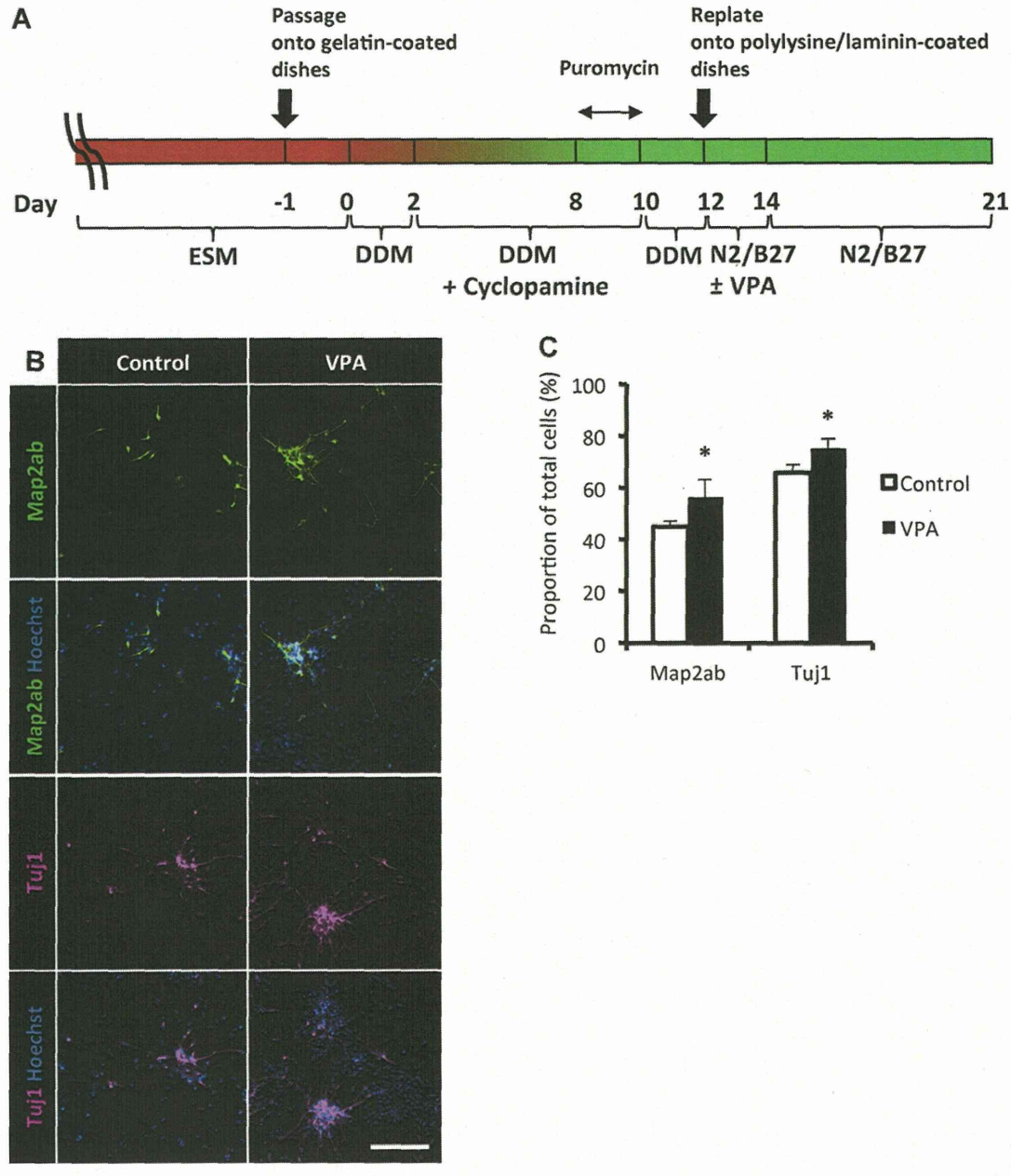

Fig. 3. Increased neurogenesis by VPA is observed even in prolonged culture. (A) Timeline of corticogenesis protocol used for late differentiation analysis. mESCs were routinely propagated and passaged to gelatin-coated dishes in embryonic stem cells medium (ESM) 1 day before neural induction (day −1). The next day (day 0), medium was changed to chemically defined default medium (DDM) and cyclopamine was added from differentiation day 2 to day 10. At differentiation day 12, mESC-derived NPCs were replated to polylysine/laminin-coated dishes in N2/B27 (1:1 mixture of DDM and Neurobasal + B27). Valproic acid (VPA) was added where appropriate at differentiation day 12 and cells were harvested at differentiation day 21. (B) Representative immunostaining images from differentiation day 21 of Map2ab- and Tuj1-expressing (green and magenta, respectively) cells. Merged images with Hoechst (blue) are also shown. Map2ab and Tuj1 images were derived from double- and triple-immunostaining data of Fig. 5A and B, respectively. (C) Quantification of neuronal marker-positive cells found in B. Data are mean ± SD from at least three independent experiments. $^*P < 0.05$ (Student's *t*-test). Scale bar is 100 μm. (For interpretation of the references to color in this figure legend, the reader is referred to the web version of the article.)

certain aspects of cortical neurogenesis *in vitro* (Eiraku et al., 2008; Gaspard et al., 2008), the generation of superficial-layer neurons in those studies was very limited.

In the present study, we have demonstrated that transient HDAC inhibition by VPA in 46C mESC-derived NPCs enhances their neuronal differentiation (Fig. 2D and E). This has been reported previously in several studies using different types of NPCs (Hsieh et al., 2004; Murabe et al., 2007; Yu et al., 2009). Using an mESC culture system that can specifically produce and recapitulate the generation of cortical-layer neurons (Gaspard et al., 2008, 2009), we further showed that the increasing neuronal population after VPA treatment includes a higher proportion of superficial-layer neurons (Cux1+) (Fig. 4B and D), accompanied by a decreasing proportion of early-born or deep-layer neurons (reelin+, Ctip2+) (Fig. 4A and C). Therefore, it is conceivable that VPA enhances the temporal progression of some of deep-layer-producing NPCs into superficial-layer-producing NPCs during the time when VPA was being supplied to the culture. The residual NPCs retained this temporal progression even when VPA was withdrawn from the culture, because we still observed the same proportion of all cortical

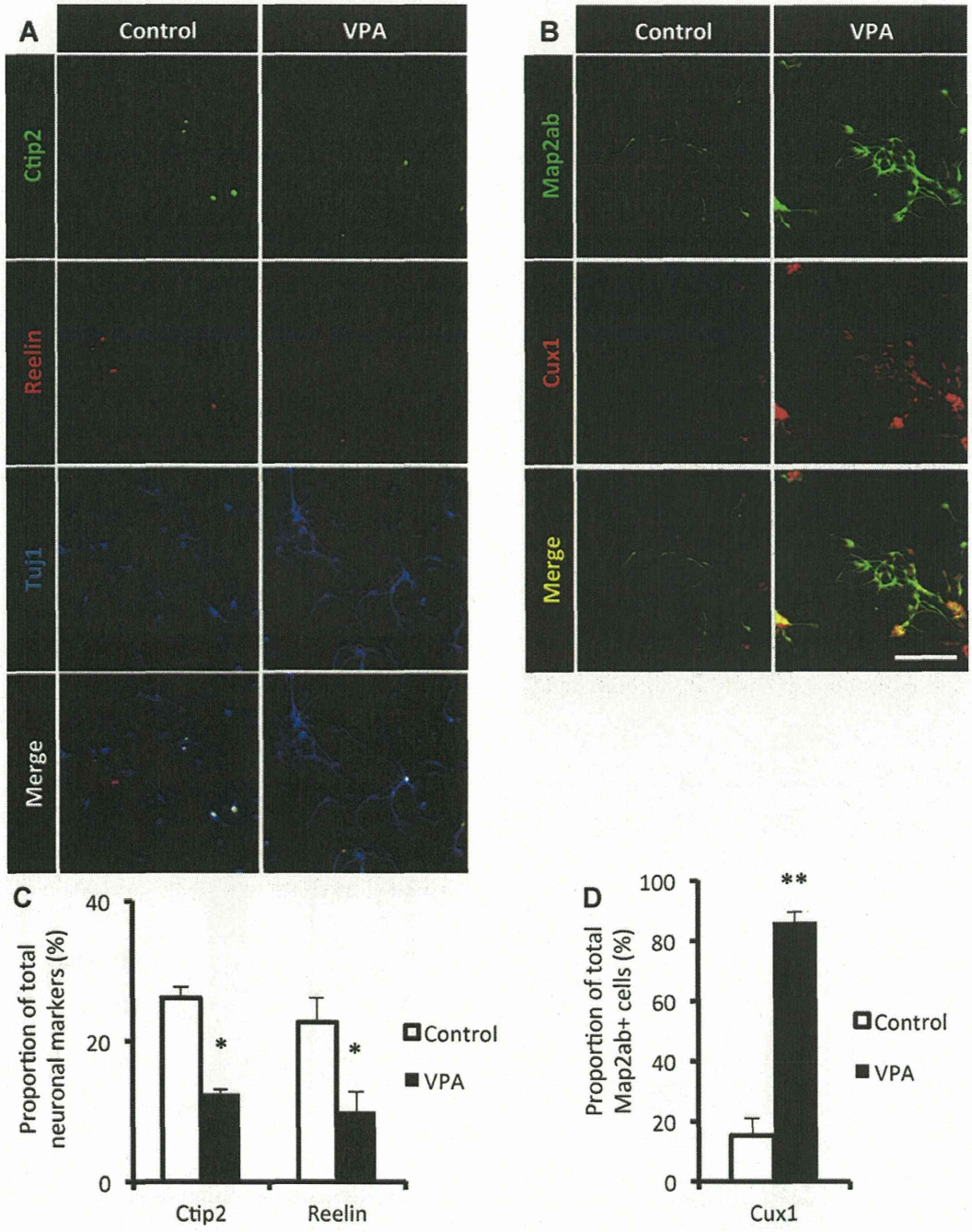

Fig. 4. VPA induces the production of superficial-layer neurons. (A and B) Representative immunostaining images from differentiation day 14, as in Fig. 2A, for Ctip2-, reelin- and Tuj1-expressing (green, red, and blue, respectively, in A), and Map2ab- and Cux1-expressing (green and red, respectively, in B) cells. Merged images are also shown. Hoechst staining can be found in Fig. 2D. Quantification of cortical layer marker-positive cells among neuronal marker-expressing cells for early-born or deep-layer (C) and superficial-layer neurons (D). Data are mean ± SD from at least three independent experiments. $^{*}P < 0.05$, $^{**}P < 0.001$ (Student's *t*-test). Scale bar is 100 μm. (For interpretation of the references to color in this figure legend, the reader is referred to the web version of the article.)

markers even at differentiation day 21, 7 days after VPA treatment was terminated (Fig. 5A–D).

Elucidating the mechanisms that lead to the enhanced progression of NPCs from producing deep-layer neurons to producing superficial-layer neurons after transient VPA treatment is an important challenge for future study. It has been proposed that the zinc-finger transcription factor *Fezf2*, which acts upstream of *Ctip2*, plays an important role in the specification of deep-layer neurons (Chen et al., 2008; Leone et al., 2008). VPA might repress *Fezf2* directly or indirectly in our culture system, which could in turn decrease the generation of deep-layer neurons and release the inhibition of upper-layer neuron production. This scenario is plausible, since VPA treatment of mouse embryos reduces levels of *Fezf2* mRNA in the forebrain (B.J. and K.N., unpublished data), and since there was an increase of Tbr1-positive cells in our culture after VPA treatment (data not shown). It has been reported recently that Tbr1 can act as a direct transcriptional repressor for *Fezf2* (Han et al., 2011).

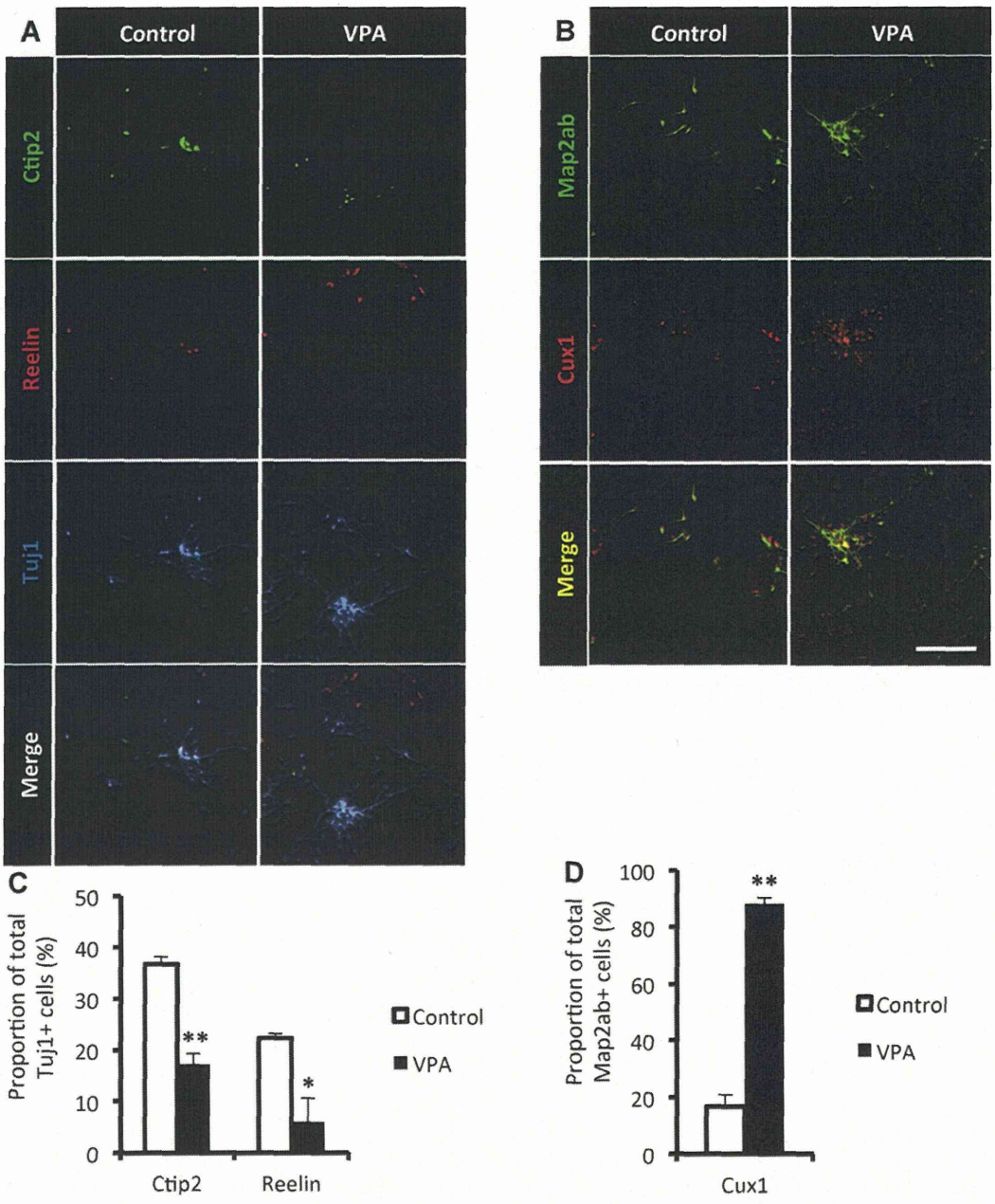

Fig. 5. Increased generation of superficial-layer neurons by VPA is observed even in prolonged culture. (A and B) Representative immunostaining images from differentiation day 21, as in Fig. 3A, for Ctip2-, reelin- and Tuj1-expressing (green, red, and blue, respectively, in A), and Map2ab- and Cux1-expressing (green and red, respectively, in B) cells. Merged images are also shown. Hoechst staining can be found in Fig. 3B. Quantification of cortical layer marker-positive cells among neuronal marker-expressing cells for early-born or deep-layer (C) and superficial-layer neurons (D). Data are mean ± SD from at least three independent experiments. $^{*}P < 0.05$, $^{**}P < 0.001$ (Student's *t*-test). Scale bar is 100 μm. (For interpretation of the references to color in this figure legend, the reader is referred to the web version of the article.)

Our results suggest that histone acetylation plays important roles in the production of superficial-layer neurons in an adherent monolayer system. Similar efficient production of superficial-layer neurons from mESCs was also recently reported in a study of modified embryoid body (EB) formation (Eiraku et al., 2008). It is tempting to hypothesize that in the EB, high levels of histone acetylation occur and persist until late differentiation to help ensure the generation of superficial layer neurons. Nevertheless, generation of cortical neurons from human (h)ESCs using the same EB method was skewed toward deep-layer identity (Eiraku et al., 2008), and both mESCs and hESCs failed to recapitulate the same inside-out pattern of cortical neurogenesis observed in the developing cortex (Au and Fishell, 2008; Gaspard and Vanderhaeghen, 2010). It will be of interest to explore the effects of increasing histone acetylation by VPA treatment on the production of superficial-layer neurons in hESCs, and whether histone acetylation plays a role in the inside-out mode of cortical neurogenesis.

Acknowledgments

We thank Y. Bessho, T. Matsui, Y. Nakahata, J. Kohyama, T. Takizawa and M. Namihira for valuable discussions. We also thank I. Smith for critical reading of the manuscript. We are very grateful to M. Tano for her excellent secretarial assistance and other

laboratory members for technical help. This research was supported in part by Grant-in-Aid for Scientific Research on Innovative Area: NAIST Global COE Program (Frontier Biosciences: Strategies for survival and adaptation in a changing global environment) from the Ministry of Education, Culture, Sports, Science and Technology of Japan; Grant-in-Aid for Scientific Research on Innovative Area: Neural Diversity and Neocortical Organization from the Ministry of Education, Culture, Sports, Science and Technology of Japan; Health Sciences Research Grants from the Ministry of Health, Labour and Welfare, Japan; and Research Fellowships for Young Scientists from the Japan Society for the Promotion of Science.

References

Abranches, E., Silva, M., Pradier, L., Schulz, H., Hummel, O., Henrique, D., Bekman, E., 2009. Neural differentiation of embryonic stem cells *in vitro*: a road map to neurogenesis in the embryo. PLoS ONE 4, e6286.

Au, E., Fishell, G., 2008. Cortex shatters the glass ceiling. Cell Stem Cell 3, 472–474.

Bain, G., Kitchens, D., Yao, M., Huettner, J.E., Gottlieb, D.I., 1995. Embryonic stem cells express neuronal properties *in vitro*. Dev. Biol. 168, 342–357.

Balasubramaniyan, V., Boddeke, E., Bakels, R., Küst, B., Kooistra, S., Veneman, A., Copray, S., 2006. Effects of histone deacetylation inhibition on neuronal differentiation of embryonic mouse neural stem cells. Neuroscience 143, 939–951.

Chen, B., Wang, S.S., Hattox, A.M., Rayburn, H., Nelson, S.B., McConnell, S.K., 2008. The Fezf2-Ctip2 genetic pathway regulates the fate choice of subcortical projection neurons in the developing cerebral cortex. Proc. Natl. Acad. Sci. U. S. A. 105, 11382–11387.

Conti, L., Pollard, S.M., Gorba, T., Reitano, E., Toselli, M., Biella, G., Sun, Y., Sanzone, S., Ying, Q.L., Cattaneo, E., Smith, A., 2005. Niche-independent symmetrical self-renewal of a mammalian tissue stem cell. PLoS Biol. 3, e283.

Eiraku, M., Watanabe, K., Matsuo-Takasaki, M., Kawada, M., Yonemura, S., Matsumura, M., Wataya, T., Nishiyama, A., Muguruma, K., Sasai, Y., 2008. Self-organized formation of polarized cortical tissues from ESCs and its active manipulation by extrinsic signals. Cell Stem Cell 3, 519–532.

Finlay, B.L., Darlington, R.B., 1995. Linked regularities in the development and evolution of mammalian brains. Science 268, 1578–1584.

Gaspard, N., Bouschet, T., Hourez, R., Dimidschstein, J., Naeije, G., van den Ameele, J., Espuny-Camacho, I., Herpoel, A., Passante, L., Schiffmann, S.N., Gaillard, A., Vanderhaeghen, P., 2008. An intrinsic mechanism of corticogenesis from embryonic stem cells. Nature 455, 351–357.

Gaspard, N., Bouschet, T., Herpoel, A., Naeije, G., van den Ameele, J., Vanderhaeghen, P., 2009. Generation of cortical neurons from mouse embryonic stem cells. Nat. Protoc. 4, 1454–1463.

Gaspard, N., Vanderhaeghen, P., 2010. Mechanisms of neural specification from embryonic stem cells. Curr. Opin. Neurobiol. 20, 37–43.

Guillemot, F., Molnár, Z., Tarabykin, V., Stoykova, A., 2006. Molecular mechanisms of cortical differentiation. Eur. J. Neurosci. 23, 857–868.

Han, W., Kwan, K.Y., Shim, S., Lam, M.M., Shin, Y., Xu, X., Zhu, Y., Li, M., Sestan, N., 2011. TBR1 directly represses Fezf2 to control the laminar origin and development of the corticospinal tract. Proc. Natl. Acad. Sci. U. S. A. 108, 3041–3046.

Hill, R.S., Walsh, C.A., 2005. Molecular insights into human brain evolution. Nature 437, 64–67.

Hsieh, J., Nakashima, K., Kuwabara, T., Mejia, E., Gage, F.H., 2004. Histone deacetylase inhibition-mediated neuronal differentiation of multipotent adult neural progenitor cells. Proc. Natl. Acad. Sci. U. S. A. 101, 16659–16664.

Juliandi, B., Abematsu, M., Nakashima, K., 2010. Chromatin remodeling in neural stem cell differentiation. Curr. Opin. Neurobiol. 20, 408–415.

Kawasaki, H., Mizuseki, K., Nishikawa, S., Kaneko, S., Kuwana, Y., Nakanishi, S., Nishikawa, S.I., Sasai, Y., 2000. Induction of midbrain dopaminergic neurons from ES cells by stromal cell-derived inducing activity. Neuron 28, 31–40.

Leone, D.P., Srinivasan, K., Chen, B., Alcamo, E., McConnell, S.K., 2008. The determination of projection neuron identity in the developing cerebral cortex. Curr. Opin. Neurobiol. 18, 28–35.

Marin-Padilla, M., 1992. Ontogenesis of the pyramidal cell of the mammalian neocortex and developmental cytoarchitectonics: a unifying theory. J. Comp. Neurol. 321, 223–240.

Molyneaux, B.J., Arlotta, P., Menezes, J.R.L., Macklis, J.D., 2007. Neuronal subtype specification in the cerebral cortex. Nat. Rev. Neurosci. 8, 427–437.

Murabe, M., Yamauchi, J., Fujiwara, Y., Hiroyama, M., Sanbe, A., Tanoue, A., 2007. A novel embryotoxic estimation method of VPA using ES cells differentiation system. Biochem. Biophys. Res. Commun. 352, 164–169.

Pevny, L.H., Sockanathan, S., Placzek, M., Lovell-Badge, R., 1998. A role for SOX1 in neural determination. Development 125, 1967–1978.

Shen, Q., Wang, Y., Dimos, J.T., Fasano, C.A., Phoenix, T.N., Lemischka, I.R., Ivanova, N.B., Stifani, S., Morrisey, E.E., Temple, S., 2006. The timing of cortical neurogenesis is encoded within lineages of individual progenitor cells. Nat. Neurosci. 6, 743–751.

Wiles, M.V., Johansson, B.M., 1999. Embryonic stem cell development in a chemically defined medium. Exp. Cell Res. 247, 241–248.

Wonders, C.P., Anderson, S.A., 2006. The origin and specification of cortical interneurons. Nat. Rev. Neurosci. 7, 687–696.

Wood, H.B., Episkopou, V., 1999. Comparative expression of the mouse Sox1, Sox2 and Sox3 genes from pre-gastrulation to early somite stages. Mech. Dev. 86, 197–201.

Ying, Q.L., Smith, A.G., 2003. Defined conditions for neural commitment and differentiation. Methods Enzymol. 365, 327–341.

Ying, Q.L., Stavridis, M., Griffiths, D., Li, M., Smith, A., 2003. Conversion of embryonic stem cells into neuroectodermal precursors in adherent monoculture. Nat. Biotechnol. 21, 183–186.

Yu, I.T., Park, J.Y., Kim, S.H., Lee, J.S., Kim, Y.S., Son, H., 2009. Valproic acid promotes neuronal differentiation by induction of proneural factors in association with H4 acetylation. Neuropharmacology 56, 473–480.

STEM CELLS®
REGENERATIVE MEDICINE

Treatment of a Mouse Model of Spinal Cord Injury by Transplantation of Human Induced Pluripotent Stem Cell-Derived Long-Term Self-Renewing Neuroepithelial-Like Stem Cells

YUSUKE FUJIMOTO,[a,b] MASAHIKO ABEMATSU,[b] ANNA FALK,[c] KEITA TSUJIMURA,[a] TSUKASA SANOSAKA,[a] BERRY JULIANDI,[a,d] KATSUNORI SEMI,[a] MASAKAZU NAMIHIRA,[a] SETSURO KOMIYA,[b] AUSTIN SMITH,[c] KINICHI NAKASHIMA[a]

[a]Laboratory of Molecular Neuroscience, Graduate School of Biological Sciences, Nara Institute of Science and Technology, Ikoma, Japan; [b]Department of Orthopaedic Surgery, Graduate School of Medical and Dental Sciences, Kagoshima University, Kagoshima, Japan; [c]Department of Biochemistry, Wellcome Trust Centre for Stem Cell Research, Stem Cell Institute, University of Cambridge, Cambridge, United Kingdom; [d]Department of Biology, Bogor Agricultural University (IPB), Bogor, Indonesia

Key Words. Spinal cord injury • Induced pluripotent stem cells • Neural stem cells • Transplantation • Regenerative medicine

ABSTRACT

Because of their ability to self-renew, to differentiate into multiple lineages, and to migrate toward a damaged site, neural stem cells (NSCs), which can be derived from various sources such as fetal tissues and embryonic stem cells, are currently considered to be promising components of cell replacement strategies aimed at treating injuries of the central nervous system, including the spinal cord. Despite their efficiency in promoting functional recovery, these NSCs are not homogeneous and possess variable characteristics depending on their derivation protocols. The advent of induced pluripotent stem (iPS) cells has provided new prospects for regenerative medicine. We used a recently developed robust and stable protocol for the generation of long-term, self-renewing, neuroepithelial-like stem cells from human iPS cells (hiPS-lt-NES cells), which can provide a homogeneous and well-defined population of NSCs for standardized analysis. Here, we show that transplanted hiPS-lt-NES cells differentiate into neural lineages in the mouse model of spinal cord injury (SCI) and promote functional recovery of hind limb motor function. Furthermore, using two different neuronal tracers and ablation of the transplanted cells, we revealed that transplanted hiPS-lt-NES cell-derived neurons, together with the surviving endogenous neurons, contributed to restored motor function. Both types of neurons reconstructed the corticospinal tract by forming synaptic connections and integrating neuronal circuits. Our findings indicate that hiPS-lt-NES transplantation represents a promising avenue for effective cell-based treatment of SCI. STEM CELLS *2012;30:1163–1173*

Disclosure of potential conflicts of interest is found at the end of this article.

INTRODUCTION

Our current ability to reconstruct the damaged central nervous system, including spinal cord injury (SCI), is limited. SCI is one of the commonest causes of loss of movement and sensation below the level of the injured spinal cord. While partial spontaneous functional recovery has been observed in the case of moderate SCI, there is no adequate treatment to repair the injured spinal cord itself, and most patients have no therapeutic options except for general management and rehabilitation [1].

Transplantation of neural stem cells (NSCs) into the injured spinal cord has been shown to be an effective treatment [2] because of their competence to differentiate into neurons and oligodendrocytes and to secrete neurotrophic factors. Transplantation into injured spinal cords of several different types of human NS/progenitor cells, derived from human fetal tissue [3, 4] or from human embryonic stem cells (hESCs) [5, 6], promotes functional recovery in animal models. Nonetheless, the mechanism underlying such functional improvement remains to be fully elucidated.

The establishment of induced pluripotent stem cells (iPSCs) offers new prospects for regenerative therapies [7, 8]. Human iPSCs (hiPSCs) can be generated from cells in adult tissue, making it possible to create iPSCs from SCI patients themselves. From the viewpoint of ethics and host immune rejection, NSCs derived from human iPSCs (hiPS-NSCs)

Author contributions: Y.F.: conception and design, collection and assembly of data, data analysis and interpretation, and manuscript writing; A.F. and A.S.: provision of study materials; M.A., K.T., T.S., K.S., and M.N.: collection and assembly of data, data analysis and interpretation; B.J.: manuscript writing; S.K.: administrative support; K.N.: conception and design, administrative support, manuscript writing, and final approval of manuscript.

Correspondence: Kinichi Nakashima, Ph.D., Laboratory of Molecular Neuroscience, Graduate School of Biological Sciences, Nara Institute of Science and Technology, 8916-5 Takayama, Ikoma 631-0192, Japan. Telephone: 81-743-72-5471; Fax: 81-743-72-5479; e-mail: kin@bs.naist.jp. Received October 18, 2011; accepted for publication February 11, 2012; first published online in STEM CELLS *EXPRESS* March 14, 2012. 1066-5099/2012/$30.00/0 doi: 10.1002/stem.1083

appear to be an ideal resource for transplantation therapy, and the efficacy of hiPS-NSC transplantation in SCI treatment has just begun to be investigated using the mouse model of SCI [9].

We used a recently developed protocol for the generation of long-term self-renewing neuroepithelial-like stem (lt-NES) cells, which satisfy the criteria to be defined as NSCs, from several different lines of hESCs and hiPSCs [10, 11]. hiPSC-derived lt-NES (hiPS-lt-NES) cells exhibit consistent characteristics such as continuous expandability, stable neuronal and glial differentiation ability, and the capacity to generate functional mature neurons in monolayer culture. Whereas neurosphere cultures display heterogeneous character and are sensitive to variation in methodological procedures [12], monolayer cultures offer a more homogeneous and robust cell generation [13, 14].

We report here that transplanted hiPS-lt-NES cells, derived from our robust and stable monolayer cultures, have a therapeutic potential comparable to that of NSCs from human fetal spinal cord (hsp-NSCs) for SCI in the nonobese diabetic-severe combined immunodeficient (NOD-SCID) mouse model. We further show that hiPS-lt-NES cell transplantation promotes recovery of hind limb motor function through the reconstruction of the corticospinal tract (CST), and restores disrupted neuronal circuitry in a relay manner as we have previously demonstrated in a study of mouse NSC transplantation [15]. Our results suggest that hiPS-lt-NES cells represent a promising cell source for transplantation into the injured spinal cord.

Materials and Methods

Cell Culture

hsp-NSCs and hiPS-lt-NES cells were established and maintained as described previously [10, 11, 16]. The hsp-NS cell line CB660sp and hiPS-lt-NES cell line AF22 were used in the present study. hsp-NSCs were plated onto 10 μg/ml laminin (Sigma, St. Louis, MO, http://www.sigmaaldrich.com)-coated plates in maintenance medium, consisting of Euromed-N medium (Euroclone, Milano, Italy, http://www.euroclonegroup.it), 2 mM L-glutamine, 0.1 mg/ml penicillin/streptomycin (Sigma), N2 supplement (1:100), 20 ml/l B27 (all from Invitrogen, Carlsbad, CA, http://www.invitrogen.com), 10 ng/ml fibroblast growth factor (FGF, R&D Systems, Minneapolis, MN, http://www.rndsystems.com)-2, and 10 ng/ml epidermal growth factor (EGF, R&D Systems). Cells were passaged at a ratio of 1:2 every second to third day using Accutase (Sigma). hiPS-lt-NES cells were plated onto 0.1 mg/ml poly-L-ornithine and 10 μg/ml laminin (O/L, Sigma)-coated plates in maintenance medium, consisting of Dulbecco's modified Eagle's medium/F12 (Invitrogen), 2 mM L-glutamine, 1.6 mg/ml glucose, 0.1 mg/ml penicillin/streptomycin, N2 supplement (1:100), 1 μl/ml B27, 10 ng/ml FGF2 and 10 ng/ml EGF. Cells were passaged at a ratio of 1:3 every second to third day using trypsin. To induce in vitro differentiation, hiPS-lt-NES cells were plated onto an O/L-coated 35-mm dish at a density of 5×10^5 cells per dish in culture medium without both EGF and FGF, containing 1% fetal bovine serum (FBS), and cultured for 4 weeks. Half of the medium was changed every 2 days and laminin (1:500) was added to the medium once a week to prevent detachment of the cells.

Lentivirus Production and Infection of hsp-NSCs and hiPS-Lt-NES Cells

Lentivirus production and infection of cells were performed as described previously [17, 18]. hsp-NSCs and hiPS-lt-NES cells were infected with lentiviruses harboring the luciferase and green fluorescent protein (GFP) genes connected by an internal ribosomal entry site (IRES), EFp (elongation factor promoter)-luciferase-IRES-GFP (Fig. 1B). hsp-NSCs and hiPS-lt-NES cells that had undergone more than 20 passages were infected. GFP-positive cells were collected by fluorescence activated cell sorting (FACS)-Aria II CellSorter (B.D. Biosciences, San Jose, CA, http://www.bdbiosciences.com) and used for transplantation.

SCI Model and Cell Transplantation

All aspects of animal care and treatment were carried out according to the guidelines of the experimental animal care committee of Nara Institute of Science and Technology. We used female NOD-SCID mice (8-10 weeks old, weighing 18-20 g, Charles River, Osaka, Japan, http://www.crj.co.jp). Anesthetized (ketamine 50 mg/kg, xylazine 5 mg/kg, and sodium pentobarbital 20 mg/kg) mice received laminectomies and partial laminectomies at the ninth and 10th thoracic spinal vertebrae, respectively. The dorsal surface of the dura mater was exposed and SCI was induced using an SCI device (70 kdyn; Infinite Horizon impactor, Precision Systems & Instrumentation, Lexington, KY, http://www.presysin.com) as previously described [15]. The muscle and skin were closed in layers. All mice subcutaneously received gentamicin (8 mg/kg) daily. The mice underwent manual bladder evacuation once a day. Seven days after injury, mice were anesthetized and transplanted with hiPS-lt-NES cells or hsp-NSCs using a glass micropipette attached to a stereotaxic injector (Narishige, Tokyo, Japan, http://www.narishige.co.jp). The tip of the micropipette was inserted into the injury epicenter in the injured spinal cord, and 2 μl of culture medium lacking growth factors, with or without NSCs (5×10^5 μl^{-1}), was injected at a rate of 1 μl/min.

Behavioral Testing and Electrophysiological Recordings

We evaluated the motor function of the hind limbs for up to 10 weeks after injury. Two individuals, blinded to the treatment of the mice, examined motor function using the Basso Mouse Scale (BMS) locomotor rating scale [19]. Hind limb movements of the mice were captured using a high-definition digital camcorder. We edited these movies and exported movie files using editing software.

To examine signal conduction in motor pathways after SCI, motor-evoked potentials (MEPs) at 12 weeks after SCI were measured. Mice were anesthetized with intraperitoneally injected ketamine (100 mg/kg) and their heads were fixed in a stereotactic frame. The skulls were tightly fixed to a stereotaxic apparatus (Narishige). Scalping and two small craniotomies were performed with a drill over the motor cortex area (Nakanishi, Tochigi, Japan; http://www.nsk-nakanishi.co.jp). Silver ball electrodes were placed epidurally via the holes, into which mineral oil was applied. The motor cortex was stimulated with 0.2-msecond square wave pulses at a constant current of 10 mA using an electrical stimulator (SEM-3301, Nihon Kohden, Tokyo, Japan; http://www.nihonkohden.co.jp). Recording needle electrodes were inserted into the hamstring. A subcutaneous ground electrode was placed in the tail. Electrophysiological recordings were made (MED64, Alpha MED Scientific, Osaka, Japan; http://www.amedsci.com) and band-pass filtered at 1-10 kHz. Amplitudes from onset to peak of the negative deflection were measured. Latency of MEP was measured as the time interval between the end of stimulation and the onset of the first wave. Indicated values are the average of five experiments from each mouse.

Antibodies

The following antibodies were used: rabbit anti-Sox2 (1:1,000, Chemicon-Millipore, Billerica, MA, http://www.millipore.com), mouse anti-Nestin (1:250, Chemicon), rabbit anti-brain lipid-binding protein (BLBP, 1:500, Abcam, Cambridge, U.K., http://www.abcam.com), mouse anti-β-tubulin isotype III (Tuj1; 1:500,

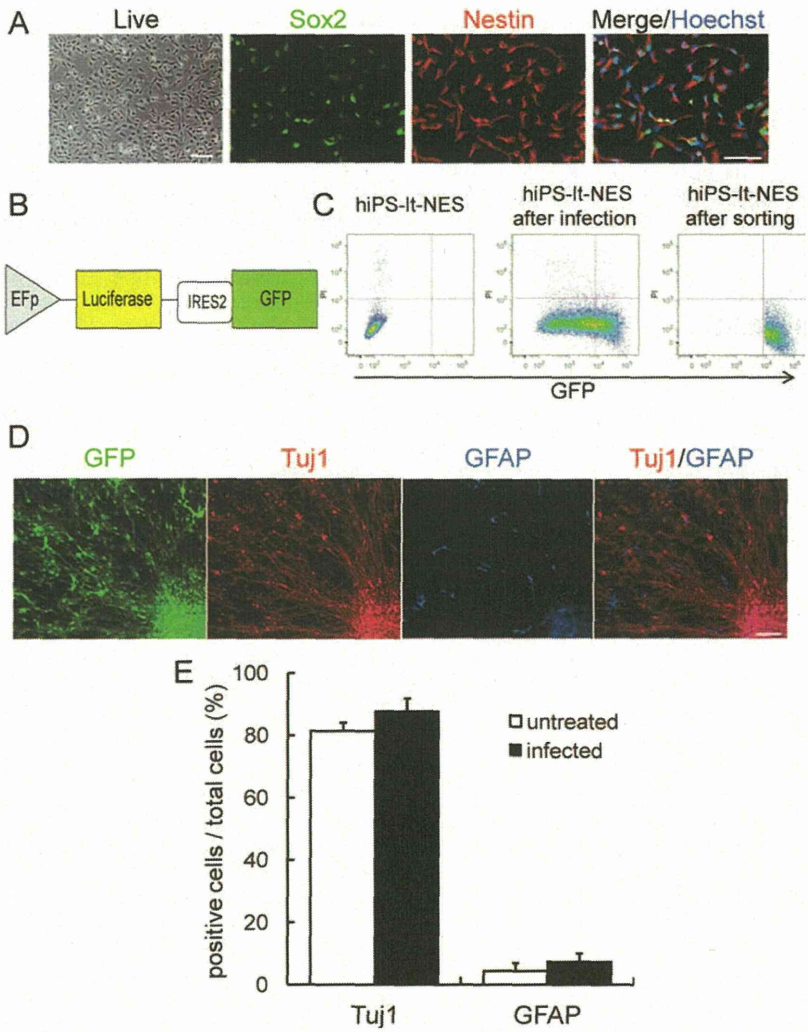

Figure 1. Characterization of hiPS-It-NES cells. **(A):** Expansion culture. hiPS-It-NES cells can be expanded continuously in the presence of both epidermal growth factor and fibroblast growth factor. hiPS-It-NES cells were uniformly immunopositive for Sox2 (green) and Nestin (red). Hoechst (blue) shows nuclear staining. **(B):** The pCSII-EFp-luciferase-IRES2-GFP construct. **(C):** Flow cytometric analysis of GFP-positive cells in hiPS-It-NES cells. Uninfected cells (left) and cells infected with lentiviruses expressing luciferase and GFP (middle) were subjected to flow cytometric analysis. GFP-positive cells in the infected cell population were sorted on the basis of GFP fluorescence and reanalyzed for GFP expression (right). **(D):** After 4 weeks in differentiation conditions, infected hiPS-It-NES cells differentiated into Tuj1-positive neurons (red) and GFAP-positive astrocytes (blue). **(E):** Quantification of neural marker-positive cells after 4 weeks' differentiation. Lentiviral infection did not influence the differentiation tendency. Data are means ± SD ($n = 3$). Scale bars = 100 μm. Abbreviations: EFp, elongation factor promoter; GFP, green fluorescent protein; GFAP, glial fibrillary acidic protein; hiPS-It-NES, human induced pluripotent stem cell-derived long-term self-renewing neuroepithelial-like stem; and IRES2, internal ribosomal entry site 2.

Sigma), rabbit anti-β-tubulin isotype III (Tuj1; 1:1,000, Covance, Madison, WI, http://www.covance.com), rabbit anti-GFP (1:1,000, Molecular Probes, Carlsbad, CA, http://probes.invitrogen.com), chick anti-GFP (1:500, Aves Labs, Tigard, OR, http://www.aveslab.com), rabbit anti-glial fibrillary acidic protein (GFAP, 1:2,000, DAKO, Carpinteria, CA, http://www.dako.com), mouse anti-human-specific GFAP (hGFAP, 1:1,000, STEM123, StemCells Science, Newark, CA, http://www.stemcellsinc.com), mouse anti-MAP2ab (1:500, Sigma), chick anti-myelin basic protein (MBP) (1:200, Aves Labs), mouse anti-adenomatous polyposis coli CC-1 (APC, 1:200, Calbiochem-Merck, Darmstadt, Germany, http://www.merckgroup.com), mouse anti-synaptophysin (1:200, Chemicon), mouse anti-Bassoon (Bsn, 1:400, Stressgen-Enzo Life Sciences, Plymouth Meeting, PA, http://www.enzolifesciences.com), mouse anti-human-specific synaptophysin (hSyn, 1:200, Chemicon), and mouse anti-NeuN (1:500, Millipore).

Immunocytochemistry

Immunocytochemistry experiments were performed as described previously [20]. Cells were washed with phosphate buffered saline (PBS) and fixed with 4% paraformaldehyde (PFA) in PBS for 10 minutes, and then washed with PBS and incubated in blocking solution (PBS containing 10% FBS and 0.1% Triton X-100). Subsequently, cells were incubated overnight at 4°C with the primary antibodies described above. After three washes in PBS, cells were incubated for 1 hour with the following secondary antibodies: FITC-conjugated donkey anti-chick/rabbit, Cy3-

conjugated donkey anti-chick/mouse/rabbit, Cy5-conjugated donkey anti-mouse/rabbit (1:500, Jackson ImmunoResearch, West Grove, PA, http://www.jacksonimmuno.com). After three washes with PBS, nuclei were stained with Hoechst (bisbenzimide H33258 fluorochrome trihydrochloride, Calbiochem-Merck). Samples were washed with PBS and mounted on glass slides with Immu-Mount (Thermo Scientific, Waltham, MA, http://www.thermoscientific.com). The cells were examined using a fluorescence microscope (Axiovert 200M, Zeiss, Jena, Germany, http://www.zeiss.com) equipped with the appropriate epifluorescence filters.

Immunohistochemistry

Animals were anesthetized and perfused with PBS followed by 4% PFA in 0.1 M PBS, pH 7.4. The spinal cords were dissected and postfixed overnight in the same fixative at 4°C. For cryosectioning, fixed tissues were cryoprotected in 10% sucrose in PBS overnight at 4°C, then in 20% sucrose in PBS overnight at 4°C, and embedded in optimal cutting temperature (OCT) compound (Tissue Tek, Sakura Finetek, Tokyo, Japan, http://www.sakura-finetek.com). Cryostat sections (20 μm) were cut and affixed to matsunami adhesive slide (MAS)-coated glass slides (Matsunami Glass, Osaka, Japan, http://www.matsunami-glass.co.jp). The sections were permeabilized in PBS-T (PBS containing 0.1% Triton X-100) for 10 minutes and blocked with 10% FBS in PBS-T for 1 hour, and then incubated overnight at 4°C with the primary antibodies described above. After three washes with PBS, they were incubated in a mixture of the secondary antibodies described above for 1 hour. After a final rinse with PBS, nuclei were stained using Hoechst. Sections were mounted and examined under a fluorescence microscope (Axiovert 200M, Zeiss) and a scanning laser confocal imaging system (LSM 710, Zeiss).

In Vivo Imaging of Transplanted Cells

In vivo imaging experiments were performed as described previously [18]. A Xenogen-IVIS 100 cooled CCD optical macroscopic imaging system (SC BioScience, Tokyo, Japan, www.scbio.co.jp) was used for bioluminescence imaging. Mice were given an intraperitoneal injection of D-luciferin (150 mg/kg) and serial images were acquired from 20 minutes after administration until the maximum intensity was obtained with the field-of-view set at 10 cm. All images were analyzed using Igor (WaveMetrics, Portland, OR, http://www.wavemetrics.com) and Xenogen Living Image software, and optical signal intensity was expressed as photon flux in units of photons/s per cm^2/steradian. To quantify the measured light, we defined regions of interest (ROIs) over the cell-implanted area and examined all values within the same ROI. The obtained photon count intensity was expressed as a percentage of the initial value.

Anterograde Labeling of the CST

Twelve weeks after injury, descending CST fibers were labeled with biotinylated dextran amine (BDA) (MW 10,000, 10% in saline, 2 μl per cortex; Molecular Probes) [21, 22] by injection into the left and right motor cortices [23]. The skulls of anesthetized mice were tightly fixed to a stereotaxic apparatus (Narishige). Scalping and craniotomy over the motor cortex area were carried out using a micromotor system (Nakanishi). The injection site was 2.1 mm posterior to the bregma, 2 mm lateral to the bregma, and 0.7 mm in depth [23]. For pressure injections with a 20-μm outer diameter glass capillary attached to a microsyringe (Narishige), we used 0.1-μl steps per minute until the desired volume (1 μl per injection site) was injected. Two weeks later, the animals were perfused and their spinal cords were fixed as described above. Sections (30 μm) were cut and used for immunohistochemistry. To visualize the BDA, a tyramide signal amplification fluorescence system (Perkin Elmer, Waltham, MA, http://www.perkinelmer.com) was used.

Visualization of Multisynaptic Neural Pathways

To visualize selective and functional transsynaptic neural pathways, wheat germ agglutinin (WGA)-expressing recombinant adenoviruses were used [24, 25]. Twelve weeks after injury, 1 μl of saline containing WGA-expressing virus at a titer of 1×10^{11} pfu/ml was injected into the bilateral motor cortices (0.5 μl per injection site). The injection site was 2.1 mm posterior to the bregma, 2 mm lateral to the bregma, and 0.7 mm in depth. Two weeks later, animals were perfused and the spinal cords were fixed as described above. Sections (15 μm) were cut and used for immunohistochemistry. Rabbit anti-WGA polyclonal antibody (3 μg/ml, Sigma) was preabsorbed with 1% acetone powder of mouse brains in blocking solution overnight at 4°C.

Ablation of Transplant-Derived Cells

Cell ablation experiments were performed as described previously [26, 27]. Diphtheria toxin (DT) was purified from conditioned medium of the PW8 strain of *Corynebacterium diphtheriae* by diethylaminoethyl Sepharose column chromatography and diluted to an appropriate concentration with saline. Seven weeks after injury, DT solution (50 μg/kg per day $\times$ 2 days) was administered by intraperitoneal injection into seven hiPS-NES cell-transplanted mice.

Statistical Analysis

We performed statistical analysis with an unpaired two-tailed Student's t test for single comparisons. For &&&BMS and BDA fiber analysis, we used repeated-measures analysis of variance (ANOVA) with Tukey-Kramer multiple comparison test at each point (Prism, GraphPad, LA Jolla, CA, http://www.graphpad.com). $p < .05$ was considered significant.

Results

Characterization of hiPS-Lt-NES Cells In Vitro

We have previously shown that hiPS-NES cells, which are reliably derived from different hiPS cell lines, exhibit consistent characteristics such as continuous expandability, stable neuronal and glial differentiation, and the capacity to generate functional mature human neurons [11]. hiPS-lt-NES cells can be expanded in the presence of FGF2 and EGF in monolayer culture, and express the NSC markers Sox2 and Nestin (Fig. 1A) and the radial glial marker BLBP (Supporting Information Fig. 1), but not the ES/iPS cell markers Oct3/4 or Nanog (not shown).

To visualize transplanted cells by both luminescence and fluorescence, hiPS-lt-NES cells were infected with lentiviruses engineered to express luciferase and GFP (Fig. 1B). Almost all hiPS-lt-NES cells were infected (Fig. 1C, middle), and we isolated only strongly GFP-expressing cells for use in subsequent in vitro and transplantation experiments (Fig. 1C, right).

We then examined whether lentiviral infection affected the differentiation potential of hiPS-lt-NES cells. Uninfected and infected hiPS-lt-NES cells were induced to differentiate by removal of growth factors and cultured in the presence of 1% FBS for 4 weeks. Both hiPS-lt-NES cell population differentiated into large and small numbers of Tuj1-positive neurons and GFAP-positive astrocytes, respectively, as observed in our previous study [11] (Fig. 1D). Quantitative analysis revealed no significant differences in the proportions of differentiated cells between uninfected and infected hiPS-lt-NES cells (Fig. 1E). Thus, we concluded that lentiviral infection did not influence the differentiation potential of hiPS-NES cells.

Transplantation of hiPS-Lt-NES Cells into the Injured Spinal Cord Improves Functional Recovery of Hind Limbs

In the present study, we used NOD-SCID mice, which are a suitable model for xenograft research because they are constitutively immunodeficient; their pathology and innate immune response after SCI are also similar to those of other mouse strains [4, 9, 28].

Previous studies have already shown that transplantation of human NSCs from fetal spinal cord or brain tissue improves locomotor functional recovery of SCI models [3, 4]. Nevertheless, only recently has the efficacy of hiPS-NSC transplantation into SCI begun to be investigated [9]. To determine whether our hiPS-lt-NES cells have a therapeutic capability, we first sought to compare the effects of these cells with those of human fetal spinal cord-derived NSCs (hsp-NSCs). Seventy-kilodyne contusive SCI was applied at the ninth thoracic vertebral level of mouse spinal cords, and 1 week later we injected medium alone (SCI control), or medium containing hsp-NSCs or hiPS-lt-NES cells, into the epicenter. We then monitored the animals' hind limb motor function using the BMS [19] for at least 8 weeks. All mice showed complete paralysis at 1-day after SCI (BMS scores were 0, Supporting Information Video 1). At 8 weeks after SCI, control mice could move their hind limbs but could not support their own weight (BMS scores were approximately 2, Supporting Information Video 2). In contrast, mice that received hsp-NSCs could touch the ground with their paws and/or support their body weight using their hind limbs (BMS scores were 3-4). The hiPS-lt-NES cell-transplanted group also showed functional recovery (BMS scores were 3-4, Supporting Information Video 3) compared to the control group, and there was no significant difference in BMS scores between the hsp-NSC- and hiPS-lt-NES cell-transplanted groups (Fig. 2A). These results indicate that hiPS-NES cells have a comparable therapeutic effect to hsp-NSCs on SCI.

Next, to evaluate the recovery of descending pathways from the motor cortex to the hind limb motor neurons, we monitored MEPs at 12 weeks after SCI. We stimulated motor cortices electrically and recorded MEP amplitudes from the hamstring muscles. The MEP amplitudes in the hiPS-NES cell-transplanted group were significantly higher than those in the SCI control group (Fig. 2B, 2C). Furthermore, the latency of MEP response in the hiPS-lt-NES cell-transplanted group was significantly shorter than that in the SCI control group (Fig. 2D). These results suggest that transplantation of hiPS-lt-NES cells into the injured spinal cord stimulates the functional recovery of hind limbs.

Transplanted hiPS-Lt-NES Cells Survive and Differentiate in the Injured Spinal Cord of NOD-SCID Mice

We have established hiPS-lt-NES cells that express luciferase and GFP, enabling us to trace the survival of the transplanted cells with a bioluminescence imaging system which detects photon signals from living cells after administration of luciferin (a substrate of luciferase) to the mice [18]. The photon signals decreased gradually after transplantation (Fig. 3A) and approximately 20% of transplanted hiPS-lt-NES cells survived in the injured spinal cord at 5 weeks after SCI (4 weeks after transplantation), whereafter the photon signals remained stable (Fig. 3B).

Using immunohistochemistry, we found that GFP-positive transplanted cells survived and migrated to both rostral and caudal areas around the lesion site in the injured spinal cord (Fig. 3C). High-magnification images showed that transplanted hiPS-lt-NES cells extended processes into both gray and white matter (Fig. 3C-1, 3C-2).

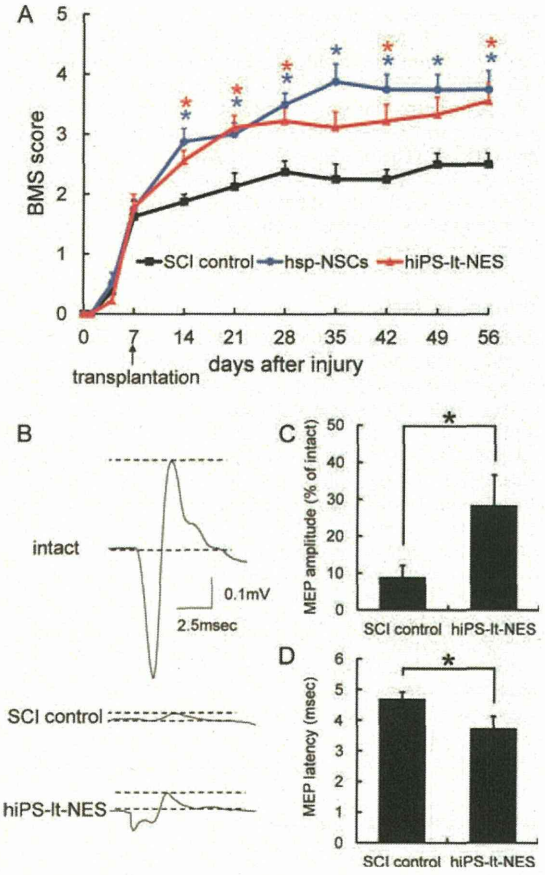

Figure 2. Transplantation of hiPS-lt-NES cells into the injured spinal cord improves functional recovery of hind limbs. **(A):** Time course of functional recovery of hind limbs after SCI. Data are means ± SEM (SCI control, $n = 8$; hsp-NSCs, $n = 8$; hiPS-lt-NES cells, $n = 9$). Mean BMS values of hsp-NSC- and hiPS-lt-NES cell-transplanted groups were compared with those of the SCI control group. *, $p < .05$. There was no significant difference between values in the hsp-NSC group and the hiPS-lt-NES cell group. **(B):** Representative MEP waves of intact, SCI control, and hiPS-lt-NES cell-treated mice at 12 weeks after injury. The motor cortices were stimulated and MEP amplitudes were recorded from hamstring muscles. Amplitudes from onset to peak of the negative deflection were measured. **(C):** Relative values of the mean MEP amplitudes. Values are expressed as percentages of those in intact mice. Mean relative MEP amplitude in the hiPS-lt-NES cell group was significantly higher than that in the SCI control group. *, $p < .05$. Data are means ± SD ($n = 3$). **(D):** Relative values of the mean MEP latency. Mean relative MEP latency in the hiPS-lt-NES cell group was significantly shorter than that in the SCI control group. *, $p < .05$. Data are means ± SD ($n = 3$). Abbreviations: BMS, Basso Mouse Scale; hiPS-lt-NES, human induced pluripotent stem cell-derived long-term self-renewing neuroepithelial-like stem; MEP, motor-evoked potential; hsp-NSC, human fetal spinal cord-derived neural stem cell; and SCI, spinal cord injury.

We then examined the differentiation of the transplanted hiPS-lt-NES cells in the injured spinal cord and found a similar differentiation tendency to that observed in vitro (Fig. 1D, 1E), with many GFP-positive transplant-derived cells having become Tuj1-positive neurons (75%) at 8 weeks after SCI (Fig. 3D–3F). Twenty percent of GFP-positive transplanted cells differentiated into GFAP-positive astrocytes, while their